pubs.acs.org/acschemicalbiology

Articles

An Irreversible Inhibitor to Probe the Role of *Streptococcus pyogenes* Cysteine Protease SpeB in Evasion of Host Complement Defenses

Jordan L. Woehl,[#] Seiya Kitamura,[#] Nicholas Dillon, Zhen Han, Landon J. Edgar, Victor Nizet, and Dennis W. Wolan*

Cite This: *ACS Chem. Biol.* 2020, 15, 2060−2069

Read Online

ACCESS | Metrics & More | Article Recommendations | Supporting Information

ABSTRACT: Members of the CA class of cysteine proteases have multifaceted roles in physiology and virulence for many bacteria. Streptococcal pyrogenic exotoxin B (SpeB) is secreted by *Streptococcus pyogenes* and implicated in the pathogenesis of the bacterium through degradation of key human immune effector proteins. Here, we developed and characterized a clickable inhibitor, **2*S*-alkyne**, based on X-ray crystallographic analysis and structure−activity relationships. Our SpeB probe showed irreversible enzyme inhibition in biochemical assays and labeled endogenous SpeB in cultured *S. pyogenes* supernatants. Importantly, application of **2*S*-alkyne** decreased *S. pyogenes* survival in the presence of human neutrophils and supports the role of SpeB-mediated proteolysis as a mechanism to limit complement-mediated host defense. We posit that our SpeB inhibitor will be a useful chemical tool to regulate, label, and quantitate secreted cysteine proteases with SpeB-like activity in complex biological samples and a lead candidate for new therapeutics designed to sensitize *S. pyogenes* to host immune clearance.

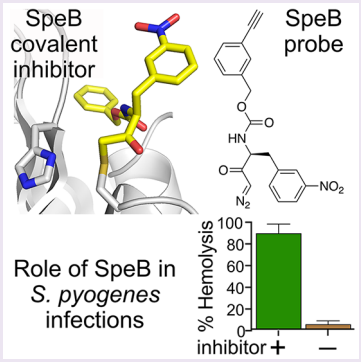

Streptococcus pyogenes is a human-specific Gram-positive bacterial pathogen that expresses several virulence factors that counteract key aspects of the innate and adaptive immune response.[1,2] Streptococcal pyrogenic exotoxin B (SpeB), a cysteine protease secreted by the majority of *S. pyogenes* strains, has been implicated in different aspects of disease pathogenesis since its discovery nearly 60 years ago.[3−5] The MEROPS Protease Database[6] categorizes SpeB as a C10 protease belonging to the papain-like clan CA. Although sequence similarity between SpeB and papain is only ∼20%, the three-dimensional organization of the SpeB catalytic residues (Cys192, His340, and Asn356) superimpose with those of papain (Cys25, His159, and Asn175). Additional highly homologous amino acids shared between the two proteases near their active sites are involved in substrate recognition.[4,7,8]

S. pyogenes causes approximately 700 million cases of pharyngitis annually and can spread systemically to cause severe invasive diseases including sepsis, necrotizing fasciitis, and streptococcal toxic shock syndrome (STSS). Including its role as the immunological trigger of rheumatic heart disease, *S. pyogenes* is responsible for approximately 500 000 deaths each year worldwide.[9,10] *S. pyogenes* interacts with host pharyngeal epithelial cells or keratinocytes through extracellular matrix binding proteins, adhesins, and invasins to establish an infection. Subsequently, the capacity of the pathogen to produce deep seated invasive infections reflects *S. pyogenes* resistance to key serum and phagocyte clearance mechanisms which normally sterilize the bloodstream.[11−15]

Complement-mediated killing is a critical aspect of the innate immune system, functioning as an early response to bacterial infection. Following initial activation of the complement cascade, bacterial cell membranes are opsonized by complement proteins C4b, C3b, and C5b, which can enhance receptor-mediated phagocytosis by neutrophils and macrophages. C5b also forms the membrane attack complex (MAC) with C6−9, directly lysing Gram-negative but not the thickened cell wall of Gram-positive bacteria, including *S. pyogenes*. Convertase formation through interactions between C4b/C2a, C3b/Factor Bb, and C3b/C4b/C2a release powerful anaphylotoxins, C3a and C5a, through the cleavage of C3 and C5. Release of these chemoattractants recruit neutrophils and other inflammatory cells to the site of infection. Interestingly, histopathological studies in human patients have often shown a surprising paucity of neutrophils at infection sites during the early stages of necrotizing fasciitis and STSS.[16,17] In addition to the production of a C5a peptidase by *S. pyogenes*,[18] sera from invasive disease patients displayed rapid degradation of complement components C3 and C3b, confirming the production of one or more C3-degrading proteases.[19] Wild-type (WT) *S. pyogenes* strains and recombinant SpeB protease (rSpeB) rapidly degrade C3b.

Accordingly, due to a decrease in neutrophil recruitment and phagocytosis, the WT Group A Streptococcus (GAS) has

Received: March 15, 2020
Accepted: July 14, 2020
Published: July 14, 2020

https://dx.doi.org/10.1021/acschembio.0c00191
ACS Chem. Biol. 2020, 15, 2060−2069

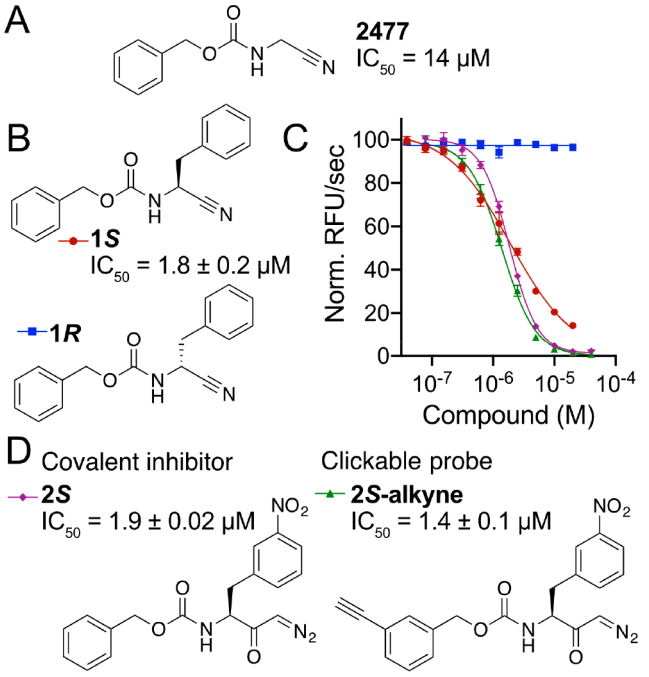

Figure 1. Development, SAR, and characterization of SpeB inhibitors. (A) Original hit molecule **2477**. (B) Structure of initial SAR compounds **1*S*** and **1*R***. (C) Dose−response curves of each compound against recombinant SpeB as measured by hydrolysis of Ac-AIK-AMC fluorescent substrate (**1*S***, red circle; **1*R***, blue square; **2*S***, purple diamond; **2*S*-alkyne**, green triangle). Each compound was assessed over a two-fold logarithmic dilution series. IC_{50} values are shown in mean ± SD ($n \geq 3$). (D) Structure of the covalent inhibitor **2*S*** and alkyne-based clickable probe **2*S*-alkyne**.

enhanced survival in human blood and murine models of infection when compared to an isogenic Δ*speB* mutant strain.[19,20] Thus, SpeB represents a potential virulence factor target, and inhibition could enhance complement-mediated host defense functions during *S. pyogenes* infection.

We previously reported the identification of a reversible small-molecule SpeB inhibitor **2477** from a high-throughput (HTS) screen against ∼16 000 commercially available compounds in the Maybridge Hitfinder library (Figure 1A).[21] Efforts to optimize **2477** derivatives for improved SpeB affinity primarily focused on additions or modifications to the phenyl ring; however, no significant improvements were identified.[21,22] We determined the high-resolution crystal structure of SpeB in complex with **2477**, and the structure identified regions of the active site that we could exploit for molecules with improved potency, including expansion from the 2-position of **2477**. Here, we present the design and development of a SpeB-targeted clickable inhibitor based on compound **2477**. We tested the utility of the compound to assist in understanding the role of SpeB in *S. pyogenes* complement and phagocyte resistance and anticipate that the probe can be employed in the identification of other CA clan proteases with SpeB-like specificity and may serve as a lead candidate for a group A streptococcus therapeutic.

RESULTS AND DISCUSSION

SpeB Inhibitor SAR. Our initial SpeB inhibitor **2477** had a modest IC_{50} value of ∼14 μM. As recently reported, initial structure−activity relationship (SAR) studies showed that addition of an (*S*)-phenylethyl group onto the 2-position (**1*S***) improved the potency to 1.8 ± 0.2 μM (Figures 1B and 1C).[22] Surprisingly, the enantiomer **1*R*** remained inactive up to 80 μM (Figures 1B, 1C, and Table 1). Evaluation of the SpeB:**2477** X-ray crystal structure suggested a potential steric clash with active site residues S282 and S280 when the phenyl ring is in the *R* conformation. In addition to this clash, we identified probable disruptions of key hydrogen bonds between the carbamate oxygen of **2477** with S282 and an active site water molecule positioned by the SpeB oxyanion hole.

Despite the lack of sequence identity, SpeB has a papain fold and is posited to be a distant homologue of the papain superfamily that includes members of the mammalian cathepsin family B, K, L, and S.[23] Potency against the structurally similar cysteine protease papaya proteinase I (papain), as well as an unrelated human cysteine protease caspase-3, showed that **1*S*** has a >20-fold selectivity for SpeB over the other two proteases (Table 1, Figure S1). We additionally assessed the ability of **1*S*** to inhibit a serine protease, as the molecule contains a core carbamate group commonly used for the inhibition of serine proteases.[24,25] Similar to papain and caspase-3, human neutrophil elastase (hNE) was also resistant to **1*S*** inhibition and resulted in >20-fold selectivity for SpeB at the highest concentration tested (40 μM) (Table 1, Figure S1). As IC_{50} values are biased to substrate concentration, we also determined the K_i of **1*S***. Varying the substrate concentration and plotting $1/v$ against the concentration of inhibitor, we determined the K_i of **1*S*** to be 1.1 ± 0.1 μM (Table 1, Figure S2).

Development of SpeB-Directed Covalent Inhibitors. Our X-ray crystal structure of SpeB bound with **2477**[21] showed that the compound is a competitive inhibitor, and previous SAR studies demonstrated that inclusion of a nitro group at the meta position on the (*S*)-phenylethyl improved the IC_{50} approximately nine-fold over the parent reversible compound **1*S***.[22] As such, all second-generation compounds included the 3-nitro *S*-phenylethyl. The nitrile moiety, located within

Table 1. Specificity and Inhibition Constants of SpeB Inhibitors

	rSpeB[b]				papain[c]		caspase-3[d]		hNE[e]	
compound	IC_{50} (μM)[a]	k_{inact} ($\times 10^{-3} s^{-1}$)	K_i (μM)	k_{inact}/K_i ($s^{-1} M^{-1}$)	IC_{50} (μM)[a]	selectivity[f]	IC_{50} (μM)[a]	selectivity[f]	IC_{50} (μM)[a]	selectivity[f]
1*S*	1.8 ± 0.2	N.D.	1.1 ± 0.1	N.D.	>40	>22	>40	>22	>40	>22
1*R*	>40	N.D.	N.D.	N.D.	>40	N.D.	>40	N.D.	>40	N.D.
2*S*	1.9 ± 0.02	4.1 ± 0.4	5.7 ± 1.2	719	32.8 ± 13	>17	>40	>21	>40	>21
2*S*-alkyne	1.4 ± 0.1	3.5 ± 0.5	4.5 ± 1.3	778	14.9 ± 1.1	>11	>40	>29	>40	>29

[a]IC_{50} values were determined using a fluorescence assay against enzymatic substrate hydrolysis. [b][rSpeB] = 20 nM; [c][papain] = 20 nM; [d][caspase-3] = 2 nM; [e][hNE] = 5 nM. Sel. [f]Selectivity is defined by the ratio of IC_{50} (SpeB) over IC_{50} (papain/caspase-3/hNE). Reported IC_{50} values are the average of triplicates with at least two datum points above and at least two below the IC_{50}.

https://dx.doi.org/10.1021/acschembio.0c00191
ACS Chem. Biol. 2020, 15, 2060−2069

hydrogen-bonding distance to the catalytic cysteine (C192), was replaced with covalent-modifying groups chloromethyl ketone (**2S-CMK**) or diazomethylketone (**2S**) to yield analogues capable of covalent SpeB inhibition (Figures 1D and S3).

We assessed the ability of **2S-CMK** and **2S** to covalently inhibit SpeB under *in vitro* conditions. Recombinant SpeB, consisting of residues 146−398 and a C-terminal His_6-tag, was incubated at 2 μM for 30 min at RT in the presence of **2S-CMK** or **2S** at concentrations 10-fold higher than their calculated IC_{50} values of 6.7 and 1.9 μM, respectively. The incubations were diluted 100-fold into an activity assay buffer consisting of PBS, pH 7.4, 0.1 mM EDTA, 10 mM DTT, and 0.1% CHAPS, and hydrolysis of the fluorogenic substrate Ac-AIK-aminomethyl coumarin (AMC) was measured.[21] We observed a return of hydrolytic activity in a dose-dependent manner in the presence of **2S-CMK**, suggesting that the molecule labels SpeB reversibly. Conversely, no change in SpeB activity was measurable in the presence of **2S**, confirming a covalent modification of the enzyme that is stable over time (Figure S3). We posit that the lack of an active site Asp residue eliminates the ability of H340 in the SpeB catalytic diad (i.e., C192, H340) to attack the halogenated carbon and displace the chlorine in **2S-CMK**, as typically observed for Cys proteases with catalytic triads. Based on these results, we continued with the characterization of **2S**.

While no improvement with respect to the affinity of **2S** for SpeB was observed (IC_{50} = 1.9 ± 0.02 μM) in comparison to **1S**, the covalent feature of the molecule reduced SpeB specificity with respect to papain from >22 to 17-fold (Figures 1D and S1, Table 1). For efficient covalent bond formation, a high potency of the initial reversible binding event (K_i) and maximum potential rate of inactivation (k_{inact}) are desired. To this end, we employed a method recently reported by Kuzmič et al. to determine K_i and k_{inact} of **2S**.[26] Using eqs 1 and 2 (see Experimental Section), we calculated the k_{inact} = 4.1 (× $10^{-3}s^{-1}$) and k_{inact}/K_i = 719 (s^{-1} M^{-1}) for compound **2S** (Table 1, Figure S4).

Crystal Structure of SpeB in Complex with 2S. We determined the X-ray crystal structure of SpeB in complex with **2S** to elucidate the covalent mechanism of inhibition. Recombinant SpeB was incubated with a 2-fold molar excess of **2S** for 2 h at 25 °C in PBS, pH 7.0 and 1 mM DTT prior to mixing with an equal volume of 0.2 M sodium nitrate, pH 5.5 and 33% (w/v) PEG 3350. The **2S**-bound SpeB structure is conserved with our previous apo and complex structures with crystallization in orthorhombic space group $P22_12_1$, an ordered leucine residue from the C-terminal His_6-tag (LEH_6), 350 water molecules, and bound nitrate molecules from the crystallization buffer. The **2477**-bound SpeB structure (PDB ID 4RKX)[21] served as the initial search model for molecular replacement, and the naïve f_0-f_c electron density map exhibited unambiguous density for **2S** located within the SpeB active site and covalently linked to C192 (Figure S5). The final R_{cryst} and R_{free} for the SpeB and **2S** cocomplex crystal structure were 15.3% and 18.9%, respectively (Table S1). **2S** was refined with 100% occupancy and has B-values similar to adjacent SpeB active site residues. The overall conformation of SpeB with **2S** is nearly identical to SpeB in complex with **2477**,[21] as is evidenced by an RMSD of 0.10 Å for all Cα atoms with a maximum deviation of 0.37 Å.

The **2S** carbamate oxygen is oriented within the SpeB oxyanion hole created by the main-chain nitrogen atoms of residues C192 and V193 (Figure 2). Importantly, the interaction with the oxyanion hole is achieved via a highly coordinated water molecule positioned by C192 and V193. The **2S** carbamate oxygen is further stabilized by the main-chain nitrogen of S282, as observed for the orientation of **2477**. The main-chain oxygen atom of residue G339 acts as a hydrogen-bond acceptor to the carbamate nitrogen of **2S**. The **2S** ketone oxygen is also highly coordinated by hydrogen bonds with C192 main-chain nitrogen and via a water-mediated interaction with the side chain of Q162 and the main-chain carbamate nitrogen of S280 (Figure 2). Both the carboxybenzyl and nitro-phenyl moieties of **2S** are nestled into regions primarily consisting of small aliphatic side chains. Our SpeB:**2S** cocomplex structure shows that the **2S** phenylethyl group extends out of the active site pocket and confirms why an *R*-enantiomer (e.g., **1R**) would result in steric clashes with the protease active site.

Development and Characterization of a Clickable SpeB Probe. With the stable covalent characteristics and X-ray structure in hand, we further modified **2S** to generate a clickable inhibitor. Based on our previous SAR and X-ray structure, we posited that the meta position of the carbamate phenyl ring would be an ideal location to append an alkyl group without compromising SpeB affinity. We converted **2S** into a clickable probe, **2S-alkyne** (Figure 1D) and the addition of an alkyne modestly improved the IC_{50} from 1.9 μM to 1.4 μM as well as yielded K_i = 4.5 μM, k_{inact} = 3.5 (× $10^{-3}s^{-1}$), and k_{inact}/K_i = 778 (s^{-1} M^{-1}) (Figures 1C, 3 and Table 1). The stable covalent interaction between **2S-alkyne** and SpeB was confirmed with the dilution assay (as described for **2S**), and no observable SpeB activity occurred upon dilution and addition of the substrate (Figure S3). The specificity of **2S-alkyne** for SpeB over papain decreased from 17-fold to 11-fold with the addition of the alkyne (Table 1, Figure S1).

The ability of **2S-alkyne** to label SpeB from *S. pyogenes* bacterial cultures was assessed. WT and Δ*speB S. pyogenes* cultures were grown overnight, bacterial cells pelleted, and the supernatants concentrated to ensure sufficient protein levels for visualization by SDS-PAGE. The concentrated *S. pyogenes* supernatant was incubated with **2S-alkyne** and followed by addition of an azide-containing fluorescent dye and the necessary azide−alkyne click chemistry materials, as described

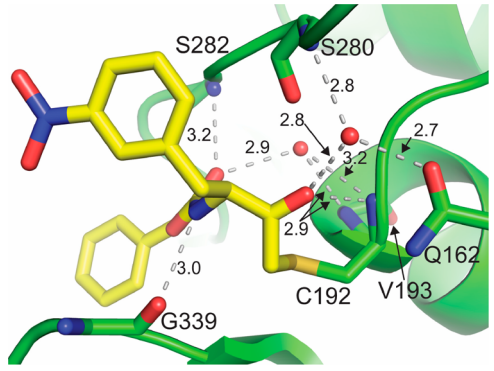

Figure 2. Crystal structure of SpeB in complex with **2S**. SpeB active site residues (green carbon) within hydrogen-bonding distance of **2S** (yellow carbon) are shown with dashed gray lines (red, oxygen; blue, nitrogen; yellow, sulfur). Waters are represented as red spheres. Continuous electron density is observed between the catalytic residue C192 and **2S**.

https://dx.doi.org/10.1021/acschembio.0c00191
ACS Chem. Biol. 2020, 15, 2060−2069

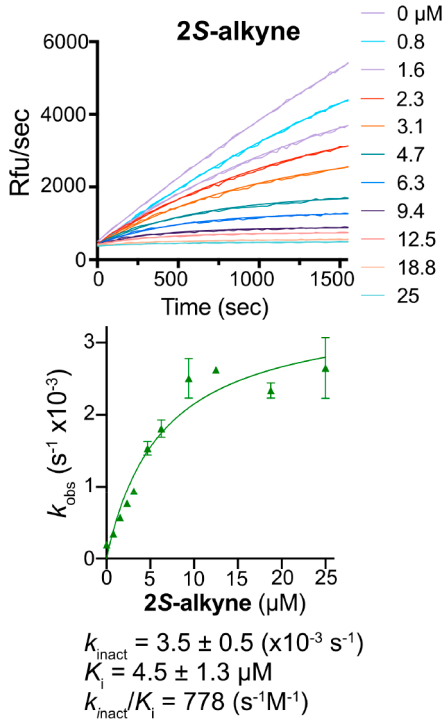

Figure 3. Dose−response curves (top) and k_{obs} (bottom) of SpeB inhibition by **2*S*-alkyne** for k_{inact} and K_i determination. Increasing concentrations of **2*S*-alkyne** were assessed against rSpeB with a constant Ac-AIK-AMC substrate concentration of 200 μM. K_i/k_{inact} values were determined using a previously described model.[26]

in the Experimental Section. The WT supernatant was resolved by SDS-PAGE (Figure 4A, top) with **2*S*-alkyne** probe labeling visualized by fluorescence of the azide-fluorophore. **2*S*-alkyne** clearly labeled *S. pyogenes*-produced SpeB, while the supernatant from Δ*speB* and DMSO-only treated samples showed no background labeling (Figure 4A, bottom).

SpeB has a relatively conserved active site architecture compared to other CA clan proteases with papain-like folds, and **2*S*-alkyne** inhibits papain with an IC_{50} value sufficient for

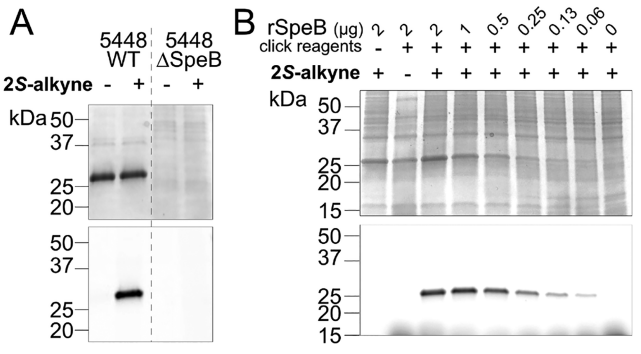

Figure 4. (A) Compound **2*S*-alkyne** labels SpeB from cultured *S. pyogenes*. Coomassie stain (above) and compound-labeled fluorescent (bottom) imaging. Incubation was followed by addition of AFDye 647 Azide with azide−alkyne click chemistry components (bottom image). WT bacterial supernatant showed specific and efficient labeling of SpeB, while the Δ*speB* strain showed no background labeling. (B) Recombinant SpeB (2 to 0.06 μg per lane) was labeled with **2*S*-alkyne** in the presence of a complex bacterial lysate (10 μg), as described in panel A with Coomassie stain (top) and in-gel fluorescence (bottom) shown.

in vitro labeling (Table 1). To this end, we evaluated the ability of **2*S*-alkyne** to label papain (Figure S6). Active papain was treated with **2*S*-alkyne** as described for labeling of *S. pyogenes*-produced SpeB, and the fluorescence image confirmed susceptibility to the probe after click conjugation of the azide fluorophore (Figure S6). While the probe did not label papain as robustly as rSpeB, these results suggest that **2*S*-alkyne** could be employed to label and/or inhibit SpeB and similar CA clan proteases in biologically relevant assays. We believe that **2*S*-alkyne** will be useful in the identification of CA clan proteases with similar substrate specificity to SpeB (i.e., papain, etc.).

We next determined the gel-based detection limits of rSpeB in the presence of a complex microbial mixture. Briefly, 10 μg of a whole-cell bacterial lysate, generated from an overnight anaerobic culture of murine fecal bacteria, was spiked with various concentrations of rSpeB (2 to 0.06 μg) (Figure 4B, top). The samples were subjected to **2*S*-alkyne** labeling, addition of an azide-containing fluorophore, and in-gel fluorescence imaging. Of note, rSpeB self-degrades when incubated with click reagents alone (e.g., absence of **2*S*-alkyne**, Figure 4B, lane 2), while addition of the probe stabilized the active state of the protease (Figure 4B, top). Recombinant SpeB is readily detected at 60 ng with in-gel fluorescence, and no background promiscuous labeling is observed. Of note, the bacterial lysates were generated from PBS-suspended cells via sonication and centrifugation to remove cellular debris. CA proteases are generally secreted and/or adhered to bacterial membranes; therefore, our microbial lysates likely contain trace amounts from this protease clan.

SpeB Inhibitors Restore Human Complement Activity and Opsonphagocytic Killing of *S. pyogenes*. Complement-mediated killing is a key mechanism of the innate immune response. Activation of the complement cascade and recognition of bacteria through opsonization of the cell membrane by C4b and C3b serve as a crucial step coordinating further immune responses. Release of the chemoattractant anaphylotoxins (C3a and C5a) following the formation of the C3/C5-convertases recruits multiple immune regulators, including (but not limited to) neutrophils, phagocytes, mast cells, and macrophages.[27−29]

Although SpeB exerts a multifaceted attack on several innate immune response effectors, two of its primary targets of degradation are C3b and properdin, each a key component of the alternative pathway of the complement.[19,20,30,31] Focusing on the complement-mediated immune response, we cultured *S. pyogenes* in the presence and absence of **1*S***, **1*R***, and **2*S*-alkyne** to gain an insight into the potential pharmacological activity of our SpeB inhibitors.

Effects of SpeB inhibition on *S. pyogenes* complement degradation were tested using well-established hemolysis assays that quantify the ability of normal human serum (NHS) complement activity to lyse 50% of rabbit erythrocytes.[32,33] In the presence of 15% NHS (that sufficiently lyses erythrocytes), 5 μM rSpeB reduced NHS hemolysis to ∼4% of the control. Co-incubation of 5 μM rSpeB with 20 μM **1*S***, **1*R*** (negative control), or **2*S*-alkyne** demonstrated that the NHS hemolytic activity was significantly restored by **2*S*-alkyne** (p-value < 0.0001, Figures 5A and S7). Of note, **1*S*** restored activity to ∼30% despite being a reversible inhibitor, and **1*R*** (inactive control) was incapable of restoring hemolytic activity (Figure 5A).

We next determined the specific mechanism by which the SpeB inhibitors restore alternative pathway complement

https://dx.doi.org/10.1021/acschembio.0c00191
ACS Chem. Biol. 2020, 15, 2060−2069

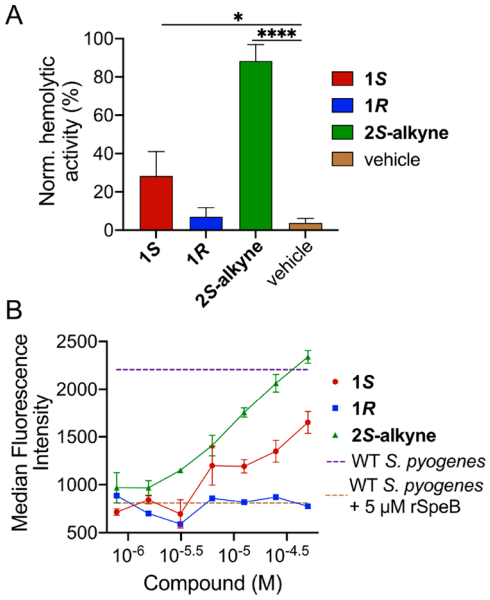

Figure 5. Compound **2*S*-alkyne** restores alternative pathway-mediated hemolysis of erythrocytes and complement-mediated opsonization. (A) The ability of **1*S***, **1*R***, and **2*S*-alkyne** to restore alternative pathway-mediated hemolysis of erythrocytes was assessed using a fixed concentration of rSpeB (5 μM), NHS [15% (v/v)], and SpeB inhibitor (20 μM). Data are represented by normalizing the signal to 15% (v/v) NHS (positive control) and GHBS° + EDTA (negative control) and are shown as mean ± SD ($n \geq 3$). *p-value = 0.024, **** = <0.0001 using a one-way ANOVA test. (B) The ability of the compounds to restore complement-mediated opsonization by C3b was analyzed by flow cytometry. *S. pyogenes* was grown overnight, diluted in assay buffer, and incubated with 10% (v/v) NHS ± 10 μM rSpeB, and C3b deposition was analyzed using an FITC-conjugated anti-C3b antibody. Compounds were added to the bacteria + rSpeB and NHS in a dose-dependent manner. Values are represented as median fluorescence intensity (MFI) and are shown as mean ± SD ($n \geq 3$).

activity. We employed an experimental system that quantifies C3b opsonization on the cellular surface of *S. pyogenes* in the presence of SpeB. Although SpeB is a secreted protease, previous research suggests that the protease can also be found associated with the bacterial cell surface.[34] To address the importance of surface-bound SpeB, we analyzed C3b deposition on both *S. pyogenes* serotype M1 WT strain (5448) and the isogenic SpeB-null strain, M1 5448 Δ*speB*.[35] Increasing concentrations of NHS were supplemented to bacterial cultures and then stained with a C3b monoclonal antibody conjugated with FITC for visualization by flow cytometry (Figure S8). Similar levels of C3b deposition were observed for both WT and Δ*speB*, suggesting that surface-bound SpeB in the WT strain (if present) does not significantly contribute to *S. pyogenes* complement evasion. Conversely, in the presence of 10% NHS, exogenously added rSpeB blocked deposition of C3b on both WT and Δ*speB S. pyogenes* strains in a dose-dependent manner (Figure S8).

We then focused on the WT *S. pyogenes* strain to determine if inhibition of SpeB activity by **1*S***, **1*R***, or **2*S*-alkyne** would restore C3b deposition on the bacterial cell membrane and downstream complement activity. **1*S***, **1*R***, or **2*S*-alkyne** were coincubated with 5 μM rSpeB and 10% NHS in the presence of WT *S. pyogenes*. Alone, rSpeB reduced C3b deposition to ∼30%; however, addition of both **1*S*** and **2*S*-alkyne** restored C3b deposition in a dose-dependent manner (Figure 5B).

We sought to determine their potential toxicity against human immune cells, Jurkat T lymphocytes.[36] Compounds **1*S*** and **1*R*** showed no measurable toxicity, while compound **2*S*-alkyne** decreased cell viability by ∼30% at a concentration of 50 μM after 48 h (Figure S9). At working concentrations for neutrophil killing assays, 40 μM, in addition to shorter assay times, Jurkat T cells showed a minimal decrease in cell viability, allowing for sufficient determination of phenotypic changes with the addition of our probe.

Restoration of complement deposition and subsequent release of the anaphylotoxins C3a and C5a mediate neutrophil chemotaxis to the site of infection and promote several mechanisms of bacteria killing,[27] including: (1) phagocytosis by recognition of opsonized bacteria and intracellular degradation via NADPH oxygenase-dependent mechanisms or antibacterial proteins;[37,38] (2) release of reactive oxygen species and cytokines to kill pathogens extracellularly (and recruit additional leukocytes);[39] or (3) release of neutrophil extracellular traps (NETs) with embedded enzymes such as myeloperoxidases (MPO) and neutral serine proteases (NSPs) that immobilize and kill pathogens.[40,41] Considering that SpeB promotes *S. pyogenes* virulence through disruption of host effector killing and that the absence of the protease does not impact on bacterial growth during *in vitro* culture, proof-of-principle of the therapeutic utility of **1*S***, **1*R***, or **2*S*-alkyne** must be examined in phagocytic killing assay. We infected freshly isolated human neutrophils with either WT *S. pyogenes* strain (5448) or its isogenic Δ*speB* mutant strain in the presence/absence of HNS and/or *S. pyogenes* culture supernatant. The SpeB producing WT 5448 strain was impervious to neutrophil killing in each of the conditions tested (Figure 6A), while loss of SpeB production sensitized the 5448 Δ*speB* strain to neutrophil killing in the presence of both HNS and supernatant (Figure 6B), confirming a contribution of the protease to phagocyte resistance. The therapeutic utility of **1*S***, **1*R***, or **2*S*-alkyne** for sensitizing *S. pyogenes* to neutrophil killing was then tested. With 40 μM concentration of inhibitor, neutrophil killing of WT *S. pyogenes* was increased by approximately 18% by **1*S*** and 28% by **2*S*** compared to no drug treatment (Figure 6C). Neither compound **1*S*** nor **2*S*** further increased neutrophil killing of the 5448 Δ*speB* strain (Figure 6D), attributing its therapeutic activity to the targeted protease.

CONCLUSIONS

The multifaceted effects of SpeB expression on the pathogenesis of *S. pyogenes* have been explored since its discovery nearly 60 years ago. Current methodologies have employed peptide derivative-based probes and mRNA levels for understanding expression levels and proteolytic activity throughout the course of infection. We present the design, development, and biological validation of a CA clan small-molecule covalent inhibitor. Optimization of our original hit compound **2477** via the addition of a diazoketone for covalent modification of the active site cysteine (C192) residue and attachment of an alkyne resulted in **2*S*-alkyne**. With this molecule, we can now detect SpeB expression at the protein level in biologically relevant settings. In addition, application of our SpeB inhibitors restored C3b deposition on the bacterial cell membrane that promoted complement activity and neutrophil killing, potentially providing an avenue for the development of

https://dx.doi.org/10.1021/acschembio.0c00191
ACS Chem. Biol. 2020, 15, 2060−2069

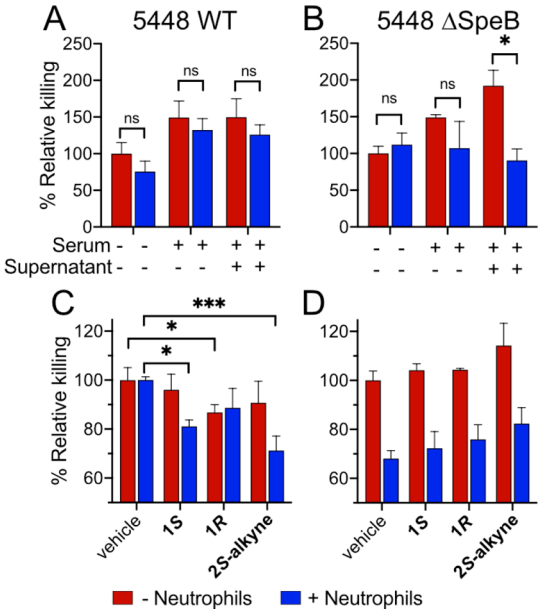

Figure 6. Compounds **1*S*** and **2*S*-alkyne** enhance neutrophil killing through selective inhibition of SpeB. Neutrophil killing assays were established for *S. pyogenes* strains (A) WT and (B) Δ*speB*, which incorporated neutrophils, fresh NHS, and bacterial culture supernatant. Percent relative killing was calculated via comparison to the unamended, no neutrophil control. Statistics were conducted by *t* tests using the Holm−Sidak method for multiple comparisons. The capacity of compounds **1*S***, **1*R***, and **2*S*-alkyne** at 40 μM to elicit neutrophil killing in the presence of NHS and bacterial supernatant was assessed against (C) WT and (D) Δ*speB*. Percent relative killing was calculated via comparison to the amended untreated, no neutrophil control. Statistical significance was calculated using a one-way ANOVA with the Dunnett correction for multiple comparisons. Significance is defined as **p*-value = <0.0332, ** = <0.0021, and *** = <0.0002. There were no statistically significant differences across conditions in panel D. All experiments were conducted in triplicate.

a therapeutically active SpeB inhibitor. We posit that **2*S*-alkyne** will also aid in the elucidation of other CA clan cysteine proteases from complex microbial mixtures.

EXPERIMENTAL SECTION

Protein Preparation and Bacterial Strains. *S. pyogenes* 10782 zymogen SpeB clone (residues 28−398) was overexpressed and purified as a C-terminal His_6-tag fusion from *E. coli* BL21DE3 (Strategene) in a pET23b vector (Novagen), as previously described.[21,42] Caspase-3 was expressed and purified as previously described.[43] Papain was purchased from MP Biomedicals, reconstituted, and purified by size-exclusion chromatography. Human sputum leucocyte elastase was purchased from Elastin Products Company, Inc. and human complement C3 and C3b were purchased from Complement Technologies. *Streptococcus pyogenes* serotype M1 (strain 5448), WT or Δ*speB*, was grown in Todd-Hewitt medium (HiMedia Laboratories) supplemented with 0.2% yeast extract (Difco) (THY media) or in C medium which consists of 0.5% Proteose Peptone #3 (Hardy Diagnostics), 1.5% yeast extract, 10 mM K_2HPO_4, 0.4 mM $MgSO_4$, 17 mM NaCl, adjusted to pH 7.5.[44]

Enzyme Assays and IC_{50} Determination. Assays were performed as previously described.[21,22,42,45,46] Briefly, rSpeB (20 nM), papain (20 nM), or caspase-3 (2 nM) was incubated in the presence of increasing amounts of inhibitor in a reaction buffer consisting of PBS, pH 7.4, 0.1 mM EDTA, 10 mM DTT, and 0.1% CHAPS and incubated for 10 min at 25 °C. Ac-AIK-AMC (SpeB and papain) (12.5 μM) or Ac-DEVD-2-aminoacridone (AMAC) (caspase-3) (100 μM) were added, and the rate of substrate hydrolysis was measured by increased (Ac-AIK-AMC)/decreased (Ac-DEVD-AMAC) fluorescence at 30 s intervals for 15 min in 96-well plates on a PerkinElmer EnVision or BioTek Synergy H1 microplate reader. hNE (5 nM) was incubated in the presence of increasing amounts of inhibitor in a reaction buffer consisting of PBS, pH 7.4 and 0.05% Nonidet P40 Substitute (Sigma) and incubated for 10 min at 25 °C. MeOSuc-AAPV-AMC (50 μM) was added, and the rate of substrate hydrolysis was measured by increased fluorescence similar to the above conditions. IC_{50} values were determined using GraphPad Prism software (GraphPad, Inc.).

k_{inact}/K_i Determination. Assays were performed as previously described.[21,45] Ac-AIK-AMC (100 μM) was mixed in the presence of increasing amounts of inhibitor in the above reaction buffer. rSpeB (20 nM) was added, and substrate hydrolysis was immediately measured by increased fluorescence at 30 s intervals for 30 min in 96-well plates on a PerkinElmer EnVision microplate reader. K_i/k_{inact} values were determined using the model described by Kuzmič et al. with a requirement that no "tight binding" of the small molecule and the enzyme occurs, and the enzyme concentration is lower than the dissociation constant of the initial enzyme−inhibitor complex.[26] Assay conditions satisfied the prerequisites of this method, including (1) a substrate concentration ([S]) lower than the K_M (e.g., 100 μM vs 247 μM) and (2) an enzyme concentration ([E]) much lower than K_i (e.g., 20 nM vs 5.7 μM). Calculations were performed with eqs 1 and 2 below, and graphs were generated with GraphPad Prism software (GraphPad, Inc.).

$$Y = (F_{min} + ((V_o/k_{obs})(1 - \exp(-k_{obs}x)))) \quad (1)$$

$$Y = k_{inact}(x/(x + K_i(1 + S/K_M))) \quad (2)$$

Reversibility of SpeB Inhibitors. rSpeB (2 μM) was incubated with each inhibitor (10-fold concentration of the kinetically determined IC_{50}) in the above reaction buffer for 30 min at 25 °C. Reactions were diluted 100-fold in assay buffer; Ac-AIK-AMC substrate was added, and the rate of substrate hydrolysis was measured by increased fluorescence at 30 s intervals for 15 min on a BioTek Synergy H1 microplate reader. Reversibility of the inhibitors was determined by analyzing the slope in comparison with the enzyme alone. All experiments were performed in triplicate.

Complement Hemolytic Assays. Assays were performed as previously described.[33] The ability of rSpeB to inhibit the activity of the alternative complement pathway was assessed using a modified hemolytic assay. Rabbit erythrocytes (Er) (Complement Tech) (5 ×108 cells/mL) were washed twice by centrifugation for 3 min at 500*g* at 4 °C. Cells were resuspended in GHBS° buffer consisting of 20 mM HEPES, pH 7.5, 140 mM NaCl, and 0.1% (w/v) gelatin. Reactions consisted of 100 μL total volume and began by diluting 5 μL of 0.1 M MgEGTA into 45 μL GHBS°, followed by 5 μL of 20× rSpeB at various concentrations, followed by 30 μL of 50% pooled complement human serum (NHS) (Innovative Research), and incubated for 10 min at 25 °C. Twenty-five microliters of Er was subsequently added to the mixture and the reactions were incubated at 37 °C for 30 min with intermittent agitation. Reactions were centrifuged (3 min, 500*g*) and diluted 1:5 with cold GHBS° in a 96-well flat-bottom half a rea clear microplate (Greiner Bio-One Inc.). Absorbance was measured at 405 nm using a PerkinElmer EnVision or BioTek Synergy H1 microplate reader. A well using buffer in place of rSpeB was treated as the 100% control, and the background was measured by replacing GHBS° with GHBS° + 10 mM EDTA. Percent lysis versus control was computed by normalizing the readings from each well to the background and 100% controls. All experiments were performed in triplicate.

The ability of rSpeB inhibitors to restore AP mediated hemolysis of erythrocytes was measured similarly to the above conditions. Briefly, rSpeB was added at a final concentration of 10 μM to ensure complete inhibition of AP hemolytic activity. Inhibitors, at a final concentration of 20 μM, were incubated with rSpeB for 5 min at 25 °C prior to the addition of NHS. Percent lysis was computed by normalizing the

https://dx.doi.org/10.1021/acschembio.0c00191
ACS Chem. Biol. 2020, 15, 2060−2069

readings from each well to the background and 100% controls. All experiments were performed in triplicate.

Complement Deposition on *S. pyogenes*. Assays were performed as previously described.[47,48] *S. pyogenes* WT strain 5448 or Δ*speB* was grown in THY media overnight at 37 °C. Bacteria was pelleted, supernatant removed, and resuspended in assay buffer consisting of 20 mM HEPES, pH 7.4, 140 mM NaCl, 0.5 mM $CaCl_2$, 0.25 mM $MgCl_2$, and 0.1% (w/v) BSA. rSpeB (5 μM) or rSpeB (5 μM) plus increasing concentrations of inhibitor was added to 5% NHS for 10 min at 25 °C, and this mixture was added directly to the bacteria (OD_{600} = 0.25) in a total volume of 200 μL and incubated at 37 °C without shaking for 30 min. Bacteria were centrifuged and unbound components were removed by several washes with assay buffer. Bacteria were resuspended in 100 μL of a 1:250 dilution of FITC-conjugated goat F(ab′)2 antihuman C3 (Protos Immunoresearch) and incubated at 4 °C for 30 min. Bacteria were washed three times with assay buffer and deposited C3b was quantified by flow cytometry using a BioRad ZE5 analyzer equipped with five lasers (355, 405, 488, 561, and 640 nm). Data shown as median fluorescence intensity and all experiments were performed in triplicate.

Crystallization and X-ray Data Collection. Crystals of rSpeB in complex with **2*S*** were grown by sitting drop-vapor diffusion, as previously described.[42] Briefly, inhibitor **2*S*** was added in 1.1-fold molar excess to rSpeB and incubated for 2 h at 25 °C and immediately used for cocrystallization experiments. Crystals of rSpeB in complex with **2*S*** were grown from a solution consisting of 0.2 M sodium nitrate, pH 5.5 with 33% (w/v) PEG 3350 at 4 °C by mixing equal volumes (2 μL) of rSpeB (10 mg mL^{-1}) and the reservoir solution. The His_6-tag was not removed as the protein crystallized readily.

Data for the rSpeB X-ray structure in complex with **2*S*** were collected on single, flash-cooled crystals at 100 K in a cryoprotectant consisting of mother liquor and 20% PEG 400 and were processed with HKL2000 in orthorhombic space group $P22_12_1$ (Table S1).[49] X-ray data for the **2*S***-rSpeB structure were collected to 1.58 Å resolution on beamline 11.1 at the Stanford Synchotron Radiation Lightsource (SSRL) (Menlo Park, CA). Data collection and processing statistics are summarized in Table S1.

Structure Solution and Refinement. The **2*S***-rSpeB complex structure was determined by molecular replacement (MR) with Phaser[50,51] using the previously published mature SpeB in complex with **2477** (PDB ID 4RKX)[21,42] as the initial search model. All structures were manually built with Coot[52] and iteratively refined using Phenix[53] with cycles of conventional positional refinement. TLS B-factor refinement was carried out in the last three rounds of refinement with the SpeB monomer split into five TLS groups as determined by TLS motion determination in Phenix. TLS refinement resulted in improved electron density maps with a minimal change in R_{cryst} and R_{free}. The electron density maps clearly identified that inhibitor **2*S*** was located within the SpeB active site (Figure S5). Water molecules were automatically positioned in Phenix using a 2.5σ cutoff in $f_0 - f_c$ maps and manually inspected. The final R_{cryst} and R_{free} are 15.3 and 18.9%, respectively (Table S1). The model was analyzed and validated with the PDB Validation Server prior to PDB deposition. Analysis of backbone dihedral angles with the program PROCHECK[51,54] indicated that all residues for the structures are located in the most favorable and allowed regions in the Ramachandran plot with no outliers. Coordinates and structure factors have been deposited in the PDB,[55] with accession entry 6UKD.

Cell Culture and Jurkat Cell Toxicity. Jurkat A3 cells were cultured as described by ATCC using 10% FBS and pen/strep/glutamine at 37 °C with 5% CO_2. For all experiments, Jurkat cells were grown to near confluence, harvested, and resuspended in fresh media into sterile Nunc 96-well tissue culture-treated plates at a density of 10 000 cells/well. Cells were treated with increasing concentrations of SpeB inhibitors or DMSO vehicle for 3 h and cellular viability was measured using CellTiter-Glo on PerkinElmer EnVision plate reader. Apoptosis was induced using 10 ng/mL MegaFasL (AdipoGen Life Sciences) as a positive control.

Neutrophil-Mediated Killing of *S. pyogenes*. Group A *Streptococcus pyogenes* neutrophil killing assays were carried out as previously described.[22] Briefly, GAS WT strain 5448 or 5448 Δ*speB*[35] were grown to logarithmic phase (~OD_{600} = 0.4) in Todd−Hewitt broth (Neogen 7161D) from an overnight culture. The logarithmic phase cultures were used to inoculate the testing condition media which contained 125.5 μL of Luria Broth (Criterion C6323) amended (10%) Rosewell-Park Memorial Insitute Medium (Gibco 11835-030) (RPMI+), 20% (50 μL) fresh human serum, 10% (25 μL) bacterial culture supernatant, and 40 μM of drug (1 μL) or 1 μL of DMSO for the no treatment control at 2 × 10^6 colony forming units. The test cultures were incubated for 30 min at 37 °C with 5% CO_2, and then 50 μL (~2 × 10^6) of freshly isolated human neutrophils (MOI 1), prepared as previously described,[56] were added, and after an additional 30 min, each culture was serially diluted in 1× DPBS (Corning) and spot played on Lauria Agar. Plates were incubated at 37 °C overnight for enumeration of CFU.

***In Situ* 2*S*-Alkyne Labeling of *S. pyogenes*-Secreted SpeB.** *S. pyogenes* WT strain 5448 or Δ*speB* was grown in C medium overnight at 37 °C. Bacterial cells were pelleted, the supernatant concentrated 20-fold, and buffer exchanged into PBS, pH 7.4. Forty microliters of a mixture containing *S. pyogenes* WT supernatant, Δ*speB* supernatant, and 100 μM **2*S*-alkyne** or DMSO (control) was incubated at 25 °C for 30 min. Click cocktail was added into the protein-probe mixture with final concentrations of 100 μM $CuSO_4$, 500 μM BTTAA (Click Chemistry Tools), 5 mM sodium ascorbate, and 100 μM AFDye 647 Azide (Click Chemistry Tools). Reaction mixture was incubated at 25 °C for 1 h. Thirty microliters was combined with 10 μL of SDS-PAGE loading dye. Samples were resolved on a 4−20% SDS-PAGE gradient gel, destained, and imaged using a Chemidoc MP Imaging System (Bio-Rad).

2*S*-Alkyne Labeling of rSpeB in the Presence of a Bacterial Lysate. A freshly collected fecal pellet from a 6-week old C57BL/6 mouse was cultured in 10 mL of 50% brain-heart infusion (BHI) media (Bacto) supplemented with 5 mg/L hemin, 1 mg/L menadione, and 1 g/L L-cysteine for 40 h at 37 °C under anaerobic conditions (97% nitrogen, 3% hydrogen). Cultured bacterial lysates were washed with PBS, pH 7.4, resuspended in 5 mL PBS, lysed by ultrasonication (QSonica), and clarified by centrifugation at 16 000*g* for 20 min. The supernatant protein solution was quantified with BCA and used for the labeling experiments. Recombinant SpeB (2 to 0.06 μg) was spiked into 10 μg of the cultured bacterial lysate and incubated in 10 μL with 100 μM **2*S*-alkyne** or DMSO (control) at 25 °C for 30 min. Click cocktail was added into the mixture with final concentrations of 100 μM $CuSO_4$, 500 μM BTTAA (Click Chemistry Tools), 5 mM sodium ascorbate, and 100 μM AFDye 647 Azide (Click Chemistry Tools) and incubated at 25 °C for 1 h. Twelve microliters was combined with 4 μL of SDS-PAGE loading dye. Samples were resolved on a 4−20% SDS-PAGE gradient gel, destained, and imaged using a Chemidoc MP Imaging System (Bio-Rad).

Statistical Analysis. All data are shown as mean ± SD with $n \geq 3$. *p*-Values for hemolytic assays were calculated using pair *t* tests with values <0.005 considered significant. *p*-Values for neutrophil killing assays were calculated using a one-way ANOVA with Dunnett correction, and significance was defined by * = <0.0332, ** = <0.0021, *** = <0.0002.

■ ASSOCIATED CONTENT

Supporting Information

The Supporting Information is available free of charge at https://pubs.acs.org/doi/10.1021/acschembio.0c00191.

Detailed information about synthetic procedures and X-ray crystallography statistics (PDF)

https://dx.doi.org/10.1021/acschembio.0c00191
ACS Chem. Biol. 2020, 15, 2060−2069

AUTHOR INFORMATION

Corresponding Author

Dennis W. Wolan − *Department of Molecular Medicine and Department of Integrative Structural and Computational Biology, The Scripps Research Institute, La Jolla, California 92037, United States;* orcid.org/0000-0001-9879-8353; Email: wolan@scripps.edu

Authors

Jordan L. Woehl − *Department of Molecular Medicine, The Scripps Research Institute, La Jolla, California 92037, United States*

Seiya Kitamura − *Department of Molecular Medicine, The Scripps Research Institute, La Jolla, California 92037, United States;* orcid.org/0000-0003-2453-849X

Nicholas Dillon − *Division of Host-Microbe Systems & Therapeutics, Department of Pediatrics, University of California San Diego, La Jolla, California 92037, United States*

Zhen Han − *Department of Molecular Medicine, The Scripps Research Institute, La Jolla, California 92037, United States*

Landon J. Edgar − *Department of Molecular Medicine, The Scripps Research Institute, La Jolla, California 92037, United States*

Victor Nizet − *Division of Host-Microbe Systems & Therapeutics, Department of Pediatrics and Skaggs School of Pharmacy and Pharmaceutical Sciences, University of California San Diego, La Jolla, California 92037, United States*

Complete contact information is available at: https://pubs.acs.org/10.1021/acschembio.0c00191

Author Contributions

#J.L.W. and S.K. contributed equally. J.L.W., S.K., and D.W.W. conceived the project. S.K. designed and synthesized SpeB inhibitors. J.L.W. performed kinetic screening, K_i determination, covalency tests, and hemolytic assays. S.K. and D.W.W. performed X-ray crystallography, data collection, and analysis. Flow cytometry experiments and analysis were completed by J.L.W. and L.J.E. Neutrophil killing assays were completed by N.D. Probe labeling of bacterial supernatant was completed by J.L.W. and Z.H. The manuscript was written by J.L.W. and D.W.W. with edits and contributions from all authors. All authors have given approval to the final version of the manuscript.

Funding

The authors gratefully acknowledge financial support from The Scripps Research Institute (to D.W.W.) and NIH grants R35 GM136286 (to D.W.W.), T32AI7354-27 (to J.L.W.), and R01 AI077780 (to V.N.).

Notes

The authors declare no competing financial interest.

ACKNOWLEDGMENTS

We thank I. Wilson, R. Stanfield, M. Elsliger, and X. Dai for computational assistance; H. Rosen and A. Ward for access to instrumentation; and the staff of beamline 11.1 at the Stanford Synchrotron Radiation Lightsource. We thank L. Lairson and A. Ward for access to their plate readers for kinetics screening. We thank B. Cravatt for access to his gel imager for labeling experiments. We thank A. Solania for providing purified caspase-3 and Ac-DEVD-AMAC substrate.

ABBREVIATIONS

SpeB, streptococcal pyrogenic exotoxin B; *S. pyogenes*, *Streptococcus pyogenes*; GAS, group A streptococcus; BTTAA, 2-(4-((bis((1-(*tert*-butyl)-1*H*-1,2,3-triazol-4-yl)methyl)-amino)methyl)-1*H*-1,2,3-triazol-1-yl)acetic acid; NHS, normal human serum; Er, rabbit erythrocytes; MAC, membrane attack complex; NSPs, neutrophil serine proteases; MPO, myeloperoxidase; NETs, neutrophil extracellular traps

REFERENCES

(1) Terao, Y., and Kawabata, S. (2009) Mechanisms of immune evasion by *Streptococcus pyogenes*. *Tanpakushitsu Kakusan Koso 54*, 982−7.

(2) Terao, Y. (2008) Molecular analyses of the development mechanisms of severe *Streptococcus pyogenes* infections. *Nippon Saikingaku Zasshi 63* (2−4), 391−8.

(3) Yu, C. E., and Ferretti, J. J. (1991) Frequency of the erythrogenic toxin B and C genes (speB and speC) among clinical isolates of group A streptococci. *Infect. Immun. 59* (1), 211−5.

(4) Tai, J. Y., Kortt, A. A., Liu, T. Y., and Elliott, S. D. (1976) Primary structure of streptococcal proteinase. III. Isolation of cyanogen bromide peptides: complete covalent structure of the polypeptide chain. *J. Biol. Chem. 251* (7), 1955−9.

(5) Liu, T. Y., and Elliott, S. D. (1965) Activation of streptococcal proteinase and its zymogen by bacterial cell walls. *Nature 206*, 33−4.

(6) Rawlings, N. D., Barrett, A. J., Thomas, P. D., Huang, X., Bateman, A., and Finn, R. D. (2018) The MEROPS database of proteolytic enzymes, their substrates and inhibitors in 2017 and a comparison with peptidases in the PANTHER database. *Nucleic Acids Res. 46* (D1), D624−D632.

(7) Chen, C. Y., Luo, S. C., Kuo, C. F., Lin, Y. S., Wu, J. J., Lin, M. T., Liu, C. C., Jeng, W. Y., and Chuang, W. J. (2003) Maturation processing and characterization of streptopain. *J. Biol. Chem. 278* (19), 17336−43.

(8) Vernet, T., Khouri, H. E., Laflamme, P., Tessier, D. C., Musil, R., Gour-Salin, B. J., Storer, A. C., and Thomas, D. Y. (1991) Processing of the papain precursor. Purification of the zymogen and characterization of its mechanism of processing. *J. Biol. Chem. 266* (32), 21451−7.

(9) Stevens, D. L., Tanner, M. H., Winship, J., Swarts, R., Ries, K. M., Schlievert, P. M., and Kaplan, E. (1989) Severe group A streptococcal infections associated with a toxic shock-like syndrome and scarlet fever toxin A. *N. Engl. J. Med. 321* (1), 1−7.

(10) Carapetis, J. R., Steer, A. C., Mulholland, E. K., and Weber, M. (2005) The global burden of group A streptococcal diseases. *Lancet Infect. Dis. 5* (11), 685−94.

(11) Hanski, E., and Caparon, M. (1992) Protein F, a fibronectin-binding protein, is an adhesin of the group A streptococcus *Streptococcus pyogenes*. *Proc. Natl. Acad. Sci. U. S. A. 89* (13), 6172−6.

(12) Terao, Y., Kawabata, S., Kunitomo, E., Murakami, J., Nakagawa, I., and Hamada, S. (2001) Fba, a novel fibronectin-binding protein from *Streptococcus pyogenes*, promotes bacterial entry into epithelial cells, and the fba gene is positively transcribed under the Mga regulator. *Mol. Microbiol. 42* (1), 75−86.

(13) Terao, Y., Kawabata, S., Nakata, M., Nakagawa, I., and Hamada, S. (2002) Molecular characterization of a novel fibronectin-binding protein of *Streptococcus pyogenes* strains isolated from toxic shock-like syndrome patients. *J. Biol. Chem. 277* (49), 47428−35.

(14) Terao, Y., Okamoto, S., Kataoka, K., Hamada, S., and Kawabata, S. (2005) Protective immunity against *Streptococcus pyogenes* challenge in mice after immunization with fibronectin-binding protein. *J. Infect. Dis. 192* (12), 2081−91.

(15) Cue, D., Southern, S. O., Southern, P. J., Prabhakar, J., Lorelli, W., Smallheer, J. M., Mousa, S. A., and Cleary, P. P. (2000) A nonpeptide integrin antagonist can inhibit epithelial cell ingestion of *Streptococcus pyogenes* by blocking formation of integrin $\alpha 5\beta$ 1-fibronectin-M1 protein complexes. *Proc. Natl. Acad. Sci. U. S. A. 97* (6), 2858−63.

(16) Cockerill, F. R., 3rd, Thompson, R. L., Musser, J. M., Schlievert, P. M., Talbot, J., Holley, K. E., Harmsen, W. S., Ilstrup, D. M., Kohner, P. C., Kim, M. H., Frankfort, B., Manahan, J. M., Steckelberg, J. M., Roberson, F., and Wilson, W. R. (1998) Molecular, serological, and clinical features of 16 consecutive cases of invasive streptococcal disease. *Clin. Infect. Dis. 26* (6), 1448−58.
(17) Hidalgo-Grass, C., Dan-Goor, M., Maly, A., Eran, Y., Kwinn, L. A., Nizet, V., Ravins, M., Jaffe, J., Peyser, A., Moses, A. E., and Hanski, E. (2004) Effect of a bacterial pheromone peptide on host chemokine degradation in group A streptococcal necrotising soft-tissue infections. *Lancet 363* (9410), 696−703.
(18) O'Connor, S. P., and Cleary, P. P. (1986) Localization of the streptococcal C5a peptidase to the surface of group A streptococci. *Infect. Immun. 53* (2), 432−4.
(19) Terao, Y., Mori, Y., Yamaguchi, M., Shimizu, Y., Ooe, K., Hamada, S., and Kawabata, S. (2008) Group A streptococcal cysteine protease degrades C3 (C3b) and contributes to evasion of innate immunity. *J. Biol. Chem. 283* (10), 6253−60.
(20) Potempa, M., and Potempa, J. (2012) Protease-dependent mechanisms of complement evasion by bacterial pathogens. *Biol. Chem. 393* (9), 873−88.
(21) Wang, A. Y., Gonzalez-Paez, G. E., and Wolan, D. W. (2015) Identification and co-complex structure of a new *S. pyogenes* SpeB small molecule inhibitor. *Biochemistry 54* (28), 4365−73.
(22) Kitamura, S., Zheng, Q., Woehl, J. L., Solania, A., Chen, E., Dillon, N., Hull, M., Kotaniguchi, M., Kitamura, S., Nizet, V., Sharpless, K. B., and Wolan, D. W. (2020) SuFEx-enabled high-throughput medicinal chemistry. *J. Am. Chem. Soc. 142*, 10899.
(23) Kagawa, T. F., Cooney, J. C., Baker, H. M., McSweeney, S., Liu, M., Gubba, S., Musser, J. M., and Baker, E. N. (2000) Crystal structure of the zymogen form of the group A Streptococcus virulence factor SpeB: an integrin-binding cysteine protease. *Proc. Natl. Acad. Sci. U. S. A. 97* (5), 2235−40.
(24) Alexander, J. P., and Cravatt, B. F. (2005) Mechanism of carbamate inactivation of FAAH: implications for the design of covalent inhibitors and in vivo functional probes for enzymes. *Chem. Biol. 12* (11), 1179−87.
(25) Lin, G., Chiou, S. Y., Hwu, B. C., and Hsieh, C. W. (2006) Probing structure-function relationships of serine hydrolases and proteases with carbamate and thiocarbamate inhibitors. *Protein J. 25* (1), 33−43.
(26) Kuzmic, P., Solowiej, J., and Murray, B. W. (2015) An algebraic model for the kinetics of covalent enzyme inhibition at low substrate concentrations. *Anal. Biochem. 484*, 82−90.
(27) Kolaczkowska, E., and Kubes, P. (2013) Neutrophil recruitment and function in health and inflammation. *Nat. Rev. Immunol. 13* (3), 159−75.
(28) Margraf, A., Ley, K., and Zarbock, A. (2019) Neutrophil recruitment: from model systems to tissue-specific patterns. *Trends Immunol. 40* (7), 613−634.
(29) Stapels, D. A., Geisbrecht, B. V., and Rooijakkers, S. H. (2015) Neutrophil serine proteases in antibacterial defense. *Curr. Opin. Microbiol. 23*, 42−8.
(30) Cunningham, M. W. (2000) Pathogenesis of group A streptococcal infections. *Clin. Microbiol. Rev. 13* (3), 470−511.
(31) Nelson, D. C., Garbe, J., and Collin, M. (2011) Cysteine proteinase SpeB from *Streptococcus pyogenes* - a potent modifier of immunologically important host and bacterial proteins. *Biol. Chem. 392* (12), 1077−88.
(32) Pham, C. T., Thomas, D. G., Beiser, J., Mitchell, L. M., Huang, J. L., Senpan, A., Hu, G., Gordon, M., Baker, N. A., Pan, D., Lanza, G. M., and Hourcade, D. E. (2014) Application of a hemolysis assay for analysis of complement activation by perfluorocarbon nanoparticles. *Nanomedicine 10* (3), 651−60.
(33) Summers, B. J., Garcia, B. L., Woehl, J. L., Ramyar, K. X., Yao, X., and Geisbrecht, B. V. (2015) Identification of peptidic inhibitors of the alternative complement pathway based on *Staphylococcus aureus* SCIN proteins. *Mol. Immunol. 67* (2 Pt B), 193−205.
(34) Hytonen, J., Haataja, S., Gerlach, D., Podbielski, A., and Finne, J. (2001) The SpeB virulence factor of *Streptococcus pyogenes*, a multifunctional secreted and cell surface molecule with strepadhesin, laminin-binding and cysteine protease activity. *Mol. Microbiol. 39* (2), 512−9.
(35) Aziz, R. K., Pabst, M. J., Jeng, A., Kansal, R., Low, D. E., Nizet, V., and Kotb, M. (2004) Invasive M1T1 group A Streptococcus undergoes a phase-shift in vivo to prevent proteolytic degradation of multiple virulence factors by SpeB. *Mol. Microbiol. 51* (1), 123−34.
(36) Nepali, K., Lee, H. Y., and Liou, J. P. (2019) Nitro-group-containing drugs. *J. Med. Chem. 62* (6), 2851−2893.
(37) Borregaard, N. (2010) Neutrophils, from marrow to microbes. *Immunity 33* (5), 657−70.
(38) Hager, M., Cowland, J. B., and Borregaard, N. (2010) Neutrophil granules in health and disease. *J. Intern. Med. 268* (1), 25−34.
(39) Lacy, P. (2006) Mechanisms of degranulation in neutrophils. *Allergy, Asthma, Clin. Immunol. 2* (3), 98−108.
(40) Phillipson, M., and Kubes, P. (2011) The neutrophil in vascular inflammation. *Nat. Med. 17* (11), 1381−90.
(41) Papayannopoulos, V., and Zychlinsky, A. (2009) NETs: a new strategy for using old weapons. *Trends Immunol. 30* (11), 513−21.
(42) Gonzalez-Paez, G. E., and Wolan, D. W. (2012) Ultrahigh and high resolution structures and mutational analysis of monomeric *Streptococcus pyogenes* SpeB reveal a functional role for the glycine-rich C-terminal loop. *J. Biol. Chem. 287* (29), 24412−26.
(43) Denault, J. B., and Salvesen, G. S. (2002) Expression, purification, and characterization of caspases. *Curr. Protoc. Protein Sci. 30*, 1.
(44) Lyon, W. R., Gibson, C. M., and Caparon, M. G. (1998) A role for trigger factor and an rgg-like regulator in the transcription, secretion and processing of the cysteine proteinase of *Streptococcus pyogenes*. *EMBO J. 17* (21), 6263−75.
(45) Solania, A., Gonzalez-Paez, G. E., and Wolan, D. W. (2019) Selective and rapid cell-permeable inhibitor of human caspase-3. *ACS Chem. Biol. 14* (11), 2463−70.
(46) Zheng, Q., Woehl, J. L., Kitamura, S., Santos-Martins, D., Smedley, C. J., Li, G., Forli, S., Moses, J. E., Wolan, D. W., and Sharpless, K. B. (2019) SuFEx-enabled, agnostic discovery of covalent inhibitors of human neutrophil elastase. *Proc. Natl. Acad. Sci. U. S. A. 116* (38), 18808−18814.
(47) Woehl, J. L., Stapels, D. A. C., Garcia, B. L., Ramyar, K. X., Keightley, A., Ruyken, M., Syriga, M., Sfyroera, G., Weber, A. B., Zolkiewski, M., Ricklin, D., Lambris, J. D., Rooijakkers, S. H. M., and Geisbrecht, B. V. (2014) The extracellular adherence protein from *Staphylococcus aureus* inhibits the classical and lectin pathways of complement by blocking formation of the C3 proconvertase. *J. Immunol. 193* (12), 6161−6171.
(48) Kuo, C. F., Lin, Y. S., Chuang, W. J., Wu, J. J., and Tsao, N. (2008) Degradation of complement 3 by streptococcal pyrogenic exotoxin B inhibits complement activation and neutrophil opsonophagocytosis. *Infect. Immun. 76* (3), 1163−9.
(49) Otwinowski, Z., and Minor, W. (1997) Processing of X-ray diffraction data collected in oscillation mode. *Methods Enzymol. 276*, 307−26.
(50) McCoy, A. J., Grosse-Kunstleve, R. W., Adams, P. D., Winn, M. D., Storoni, L. C., and Read, R. J. (2007) Phaser crystallographic software. *J. Appl. Crystallogr. 40* (4), 658−674.
(51) Collaborative Computational Project, Number 4. The CCP4 suite: programs for protein crystallography. *Acta Crystallogr., Sect. D: Biol. Crystallogr.* 1994, *50*, 5, 760−3.
(52) Emsley, P., Lohkamp, B., Scott, W. G., and Cowtan, K. (2010) Features and development of Coot. *Acta Crystallogr., Sect. D: Biol. Crystallogr. 66*, 486−501.
(53) Adams, P. D., Afonine, P. V., Bunkoczi, G., Chen, V. B., Davis, I. W., Echols, N., Headd, J. J., Hung, L. W., Kapral, G. J., Grosse-Kunstleve, R. W., McCoy, A. J., Moriarty, N. W., Oeffner, R., Read, R. J., Richardson, D. C., Richardson, J. S., Terwilliger, T. C., and Zwart, P. H. (2010) PHENIX: a comprehensive Python-based system for

https://dx.doi.org/10.1021/acschembio.0c00191
ACS Chem. Biol. 2020, 15, 2060−2069

macromolecular structure solution. *Acta Crystallogr., Sect. D: Biol. Crystallogr. 66*, 213−221.
(54) Laskowski, R. A., Macarthur, M. W., Moss, D. S., and Thornton, J. M. (1993) Procheck - a program to check the stereochemical quality of protein structures. *J. Appl. Crystallogr. 26*, 283−291.
(55) Berman, H. M., Westbrook, J., Feng, Z., Gilliland, G., Bhat, T. N., Weissig, H., Shindyalov, I. N., and Bourne, P. E. (2000) The Protein Data Bank. *Nucleic Acids Res. 28* (1), 235−42.
(56) Ulloa, E. R., Dillon, N., Tsunemoto, H., Pogliano, J., Sakoulas, G., and Nizet, V. (2019) Avibactam sensitizes carbapenem-resistant NDM-1-producing *Klebsiella pneumoniae* to innate immune clearance. *J. Infect. Dis. 220* (3), 484−493.

https://dx.doi.org/10.1021/acschembio.0c00191
ACS Chem. Biol. 2020, 15, 2060−2069